Available online at www.sciencedirect.com
ScienceDirect
Ceramics International 36 (2010) 2407–2413
CERAMICS INTERNATIONAL
www.elsevier.com/locate/ceramint

Development of ceramic electrochemical sensor based on $Bi_2Ru_2O_{7+x}$ – RuO_2 sub-micron oxide sensing electrode for water quality monitoring

Serge Zhuiykov *

Commonwealth Scientific Industrial Research Organisation (CSIRO), Materials Science and Engineering Division, 37 Graham Road, Highett, VIC 3190, Australia

Received 28 April 2010; received in revised form 12 May 2010; accepted 16 June 2010
Available online 3 August 2010

Abstract

Sub-micron $Bi_2Ru_2O_{7+x}$ + RuO_2 oxide sensing electrodes (SE) for water quality sensors were prepared on platinised ceramic substrate of the sensor. Their morphology was analysed by X-ray diffraction (XRD), scanning electron microscopy (SEM) and energy-dispersive X-ray analysis (EDX). Sensing properties of the $Bi_2Ru_2O_{7+x}$ + RuO_2-SE were investigated for potentiometric detection of pH and dissolved oxygen (DO) in water in the temperature range of 4–30 °C. Sensor was capable to measure DO from 0.5 to 8.0 ppm and pH from 2.0 to 13.0, respectively. The obtained results show acceptable linearity of the measuring characteristics. Long-term stability trial for $Bi_2Ru_2O_{7+x}$ + RuO_2-SE revealed that bio-fouling can be one of the main destructive factors affecting the performance of the sensors in the long run. The screen-printing technology used in the multi-sensory implementation provides fundamental properties of miniaturization, reasonable accuracy and low cost.

Keywords: Solid-state sensors; Water quality monitoring; Oxide sensing electrode; RuO_2

1. Introduction

Monitoring fresh and recycled water quality including wastewater is currently a subject of the growing concern in Australia and world-wide. Traditionally, the quality of water has been defined by the measurement of such parameters as pH, DO, total organic carbon, conductivity and turbidity at different temperatures. Up till now there have been various laboratory effective methods in terms of accuracy for the water quality monitoring. Although these methods comprise some advantages, they also show a number of drawbacks. For instance, most of these methods are mainly based on sample collection and retrospective analysis; data are usually collected only at a small number of fixed sampling locations; methods are time-consuming and may miss small-scale variations. Many of these disadvantages can be solved by the development of *in situ* remote sensing technologies. Following the increasing demand for real-time monitoring, several innovative techniques and sensor prototypes have been developed on a laboratory-scale in some universities, and some instrument manufacturers are now offering devices that perform rapid monitoring of water organic strength [1–8]. Nevertheless, there is still a gap between the R&D of new techniques and sensors and their effective implementation by the end user. In this respect there is an increasing interest in the development of multi-parametric, integrated, reliable, inexpensive, miniature ceramic sensors capable of meeting water quality control needs [9–12]. These sensors, in combination with the latest developed sensor networks, would be suitable for continuous monitoring of the water quality and would facilitate the process control.

Currently, micro-fabrication of the sensor elements including nanostructured oxide sensing electrodes and the introduction of multi-electrode assemblies using ceramic substrate are the most significant advances in the solid-state chemical sensor technology. This allows developing multi-electrode structures using batch fabrication processes capable to significantly reduce the cost of fabrication. However, the realisation of the latest semiconductor-based chemical sensors requires the

* Corresponding author. Tel.: +61 3 9252 6236.
E-mail address: serge.zhuiykov@csiro.au.

0272-8842/$36.00
doi:10.1016/j.ceramint.2010.07.013

integration, controlled deposition and the processing of a large number of different materials in the multi-layered sensor structures. Consequently, the new techniques for preparation of nanostructured SE and/or new materials used in smart devices and sensors for analytical systems, should preferably be used in order to combine new advantageous properties of the SE with available technologies of their preparation. Our previous experience with RuO_2-SE for the integrated water quality multi-sensor demonstrated that the application of this semiconductor as a SE is very promising and it can be widely used in electrochemical sensors [13–15]. On the contrary, the adhesion of RuO_2 to the ceramic sensor substrate was far from perfect. Some researchers employed different oxide materials (Pb, Mn, Ca) together with RuO_2 structure [9–11]. However, despite of good adhesion and acceptable sensitivity, these complex SE have shown poor selectivity to halides, sulphate, bromide and carbonate inions in water [9]. This was mainly caused by the presence of lead in available electrode pasters. However, due to the environmental concerns and the corresponding European Restriction of Hazardous Substances directive [16], there has been a strong drive towards removing lead from the thick-film materials during last few years.

To address the above demands for inexpensive planar sensors, carefully created composites and structures of ceramics must be preserved in the sensor structures, and the exotic combinations of the sensor SE materials have to be used in the hybrid structures of electrodes to optimize their performance, manufacturing efficiency, reliability, lifetime, cost and environmental compatibility. In short, modern SE materials and structures being produced from them are being pushed to new limits.

This paper focuses on the development of a new composite nanostructured $Bi_2Ru_2O_{7+x} + RuO_2$-SE for solid-state water quality sensor. Properties, including long-term stability, of the sensor attached with $Bi_2Ru_2O_{7+x} + RuO_2$-SE have been investigated for the duration of 18 months. This investigation has shown that new useful measuring device for processing multi-contributional signals from the complex parameters of the analysing liquid environment could be developed.

2. Experimental

$Bi_2Ru_2O_{7+x} + RuO_2$-SE were prepared from commercially available Bi_2O_3 and RuO_2 nanostructures (ABCR GmbH & Co.). All reagents for making nanostructured composite $Bi_2Ru_2O_{7+x} + RuO_2$-SE are of high-purity analytical grade and were used as received. Pt/Ag/Pd paste was supplied by Sigma–Aldrich Australia Pty. Ltd. Sensor alumina substrates were manufactured by Taylor Ceramic Engineering Pty. Ltd., Australia. Fig. 1 illustrates general view of the alumina substrate of the sensor with aperture for turbidity sensor showing two $Bi_2Ru_2O_{7+x} + RuO_2$-SEs deposited onto the ceramic substrate for pH and DO measurement, respectively. Assessment of an average particle size distribution revealed that the majority of RuO_2 nano-particles were in the range of 80–650 nm. Due to poorly crystalline nature of raw RuO_2 nano-particles [13], they were pre-treated at 1000 °C for 2 h in air for

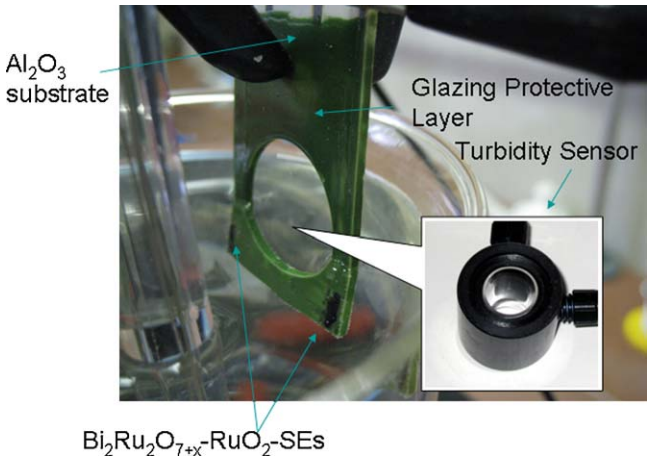

Fig. 1. View of the planar potentiometric water quality sensor with aperture for turbidity sensor.

structure stabilization before the SE development. Pt/Ag/Pd current conductors 5 μm thick were screen-printed onto the alumina substrate and were heat-treated at 900 °C for 1 h in air prior to SE deposition. Then, mixture of RuO_2 and Bi_2O_3 nano-particles was applied as a suspension in α-terpineol ($C_{10}H_{18}O$, 99.9%) onto the platinised alumina substrate and was heat-treated in two steps: heated to 400 °C at rate 65 °C/h and stabilized at 400 °C for 2 h before heating to 965 °C at rate 100 °C/h in air ensuring the development of nanostructured $Bi_2Ru_2O_{7+x} + RuO_2$-SEs [17]. Once the main phase of RuO_2 is melted, newly developed transient $Bi_2Ru_2O_{7+x}$ phase remained on the top of the RuO_2 (Fig. 2). This figure also shows that as the temperature cools down, transient liquid phase RuO_2 crystallises with appropriate steps during solidification

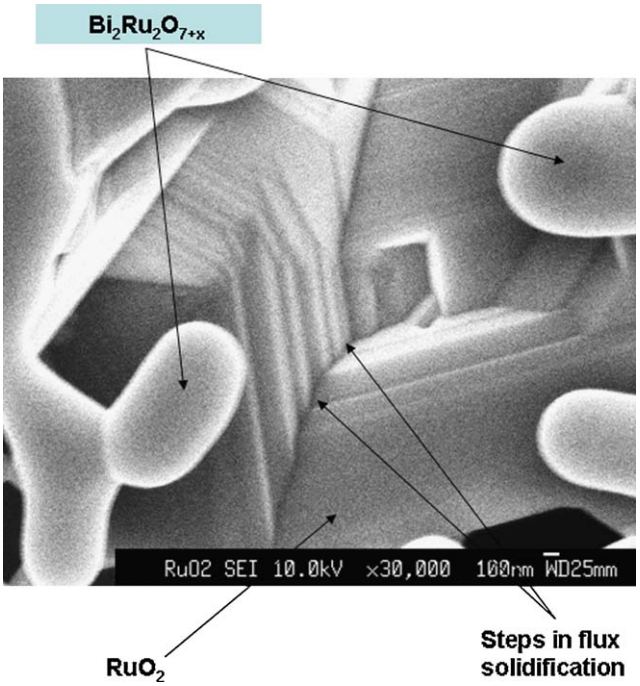

Fig. 2. SEM image of developed $Bi_2Ru_2O_{7+x} - RuO_2$ sensing electrode indicating steps in flux solidification.

providing crack-free structure. $Bi_2Ru_2O_{7+x}$ nano-particles in the range of 200–500 nm were positioned on the top of developed RuO_2. Absence of the micro-cracks in the flux structure indicates that the cooling rate was selected appropriately for this particular oxides mixture. A glazing protective layer was deposited on the alumina substrate covering both sides of substrate except the active areas of SEs and electrical contacts. The protective layer was subsequently sintered at 600 °C for 10 min. A separate standard Ag/AgCl, Cl^- reference electrode (RE) was used for pH and DO potentiometric measurements.

The sensing properties of the sub-micron $Bi_2Ru_2O_{7+x}$ + RuO_2-SEs were investigated on a water-flow apparatus equipped with a heating facility. The experimental setup enables open-circuit potentials of up to three electrodes to be collected simultaneously under various predetermined $p(O_2)$ and temperatures. The *emf* of the sensor was monitored by Keithley 2010 electrometer with a high input impedance ($>10^9$ Ω), which was connected to a PC. The temperature was carefully measured by a K-type thermocouple located adjacent to the sensor. The size of RuO_2 nano-particles of the water sensor electrodes and the surface morphology of $Bi_2Ru_2O_{7+x}$ + RuO_2-SEs were characterized by FE-SEM (JEOL JSM-6340F) and their composition was subsequently analyzed by a Wet-SEM (HITACHI, S-3000N) coupled with an energy-dispersive EDX (HORIBA, EX-220SE). XRD analyses were carried out using a Bruker D8 Advance X-Ray Diffractometer with Cu Kα (with wavelengths $K\alpha_1$ $\lambda = 1.5406$ Å, $K\alpha_2$ $\lambda = 1.544439$ Å and a $K\alpha_2$ ratio of 0.5) radiation operating at 40 kV, 40 mA and monochromatised with a graphite monochromators. XRD intensity and record was collected using a scintillation detector, and each sample was scanned over the 2θ range 10–80°.

In order to study the pH-response of $Bi_2Ru_2O_{7+x}$ + RuO_2-SEs, an initial trial was carried out in buffer solution with the fixed 8.0 pH at 23 °C. Then the pH sensing performance was subsequently tested in a stirred solution at different temperatures, where the pH changes were organised by acid–base titration. The dynamic range of this method is from 2.0 to 13.0 pH. The temperature of the solution varied from 4 to 30 °C. A calibrated commercial pH meter (HANNA Instruments, USA) was employed to monitor the pH of the solution. pH buffer solutions from 2.0 to 12.0 pH (Alfa Aesar) were used to calibrate the commercial pH meter. To test the response behaviour of the dissolved oxygen sensor, its potential response was measured as a function of DO concentration of the test solution. DO in water is usually characterized by the range of 0.5–8.0 ppm. In order to obtain the desired DO concentrations, various N_2/O_2 mixtures were pumped through the solution. A commercial dissolved oxygen analyser with auto-calibration function (HI-9142, HANNA Instruments, USA) was used to measure dissolved oxygen concentrations against the measured *emf* of integrated water sensors with nanostructured $Bi_2Ru_2O_{7+x}$ + RuO_2-SEs. The analyser was recalibrated before each measurement.

All pH and DO measurements were carried out on the sensors with freshly prepared $Bi_2Ru_2O_{7+x}$ + RuO_2-SEs, which have been kept in water for H^+ drift stabilization for at least 15 days prior to the measurements. Since DO measurements are interconnected to the pH changes of the solution, pH-response drift in time, owing to the diffusion of hydrogen ions in nanostructured RuO_2-SEs, was investigated by 30-day measurement trial in buffer solution with the fixed 7.43 pH at a temperature of 23 °C [14]. Dissolved salt solutions including potassium chloride (KCl) and bromide (KBr), lithium sulphate (Li_2SO_4), sodium sulphate (Na_2SO_4) magnesium and calcium nitrate ($Mg(NO_3)_2$ and $Ca(NO_3)_2$), as well as sodium dihydrogen phosphate (Na_2HPO_4) were used to determine the electrochemical characteristics of the SEs in terms of their cross-sensitivity, selectivity limits of detection and working concentration span. Concentrations of 10^{-7}–10^{-2} mol/l in aqueous solutions of these salts were prepared from 10^{-1} mol/l stock solutions.

3. Results and discussion

Fig. 3 shows XRD patterns of sub-micron $Bi_2Ru_2O_{7+x}$ + RuO_2-SE deposited on platinised surface of the alumina sensor substrate. Analysis of the diffraction peaks for RuO_2 illustrate that they can be indexed to the tetragonal structure of RuO_2 with a space group of *P42* and lattice parameters 4.499 Å × 4.499 Å × 3.107 Å. All well-developed diffraction peaks were narrow with high intensity indicating that ruthenium oxide nanostructure is of good crystallinity. In addition, strong well-developed peaks for $Bi_2Ru_2O_{7+x}$ phase have also been developed. The intensity of these peaks is high and they are narrow compared to those for the untreated nano-powder [13]. This result indicates that both $Bi_2Ru_2O_{7+x}$ and RuO_2 are thermally stable even at such high heat-treatment temperature (965 °C) without additional phase change, formation of any solid solution with alumina, decomposition and evaporation. Due to the relatively porous structure of the $Bi_2Ru_2O_{7+x}$ + RuO_2-SE additional peaks for alumina and Pt were also detected.

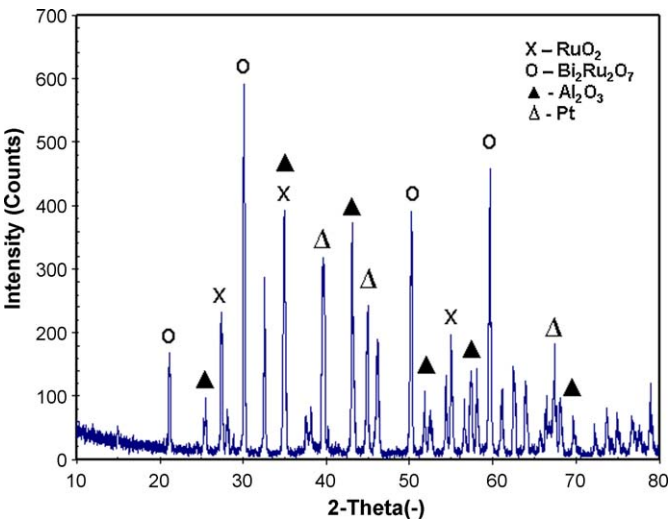

Fig. 3. XRD patterns of sub-micron $Bi_2Ru_2O_{7+x}$ + RuO_2 composite SE.

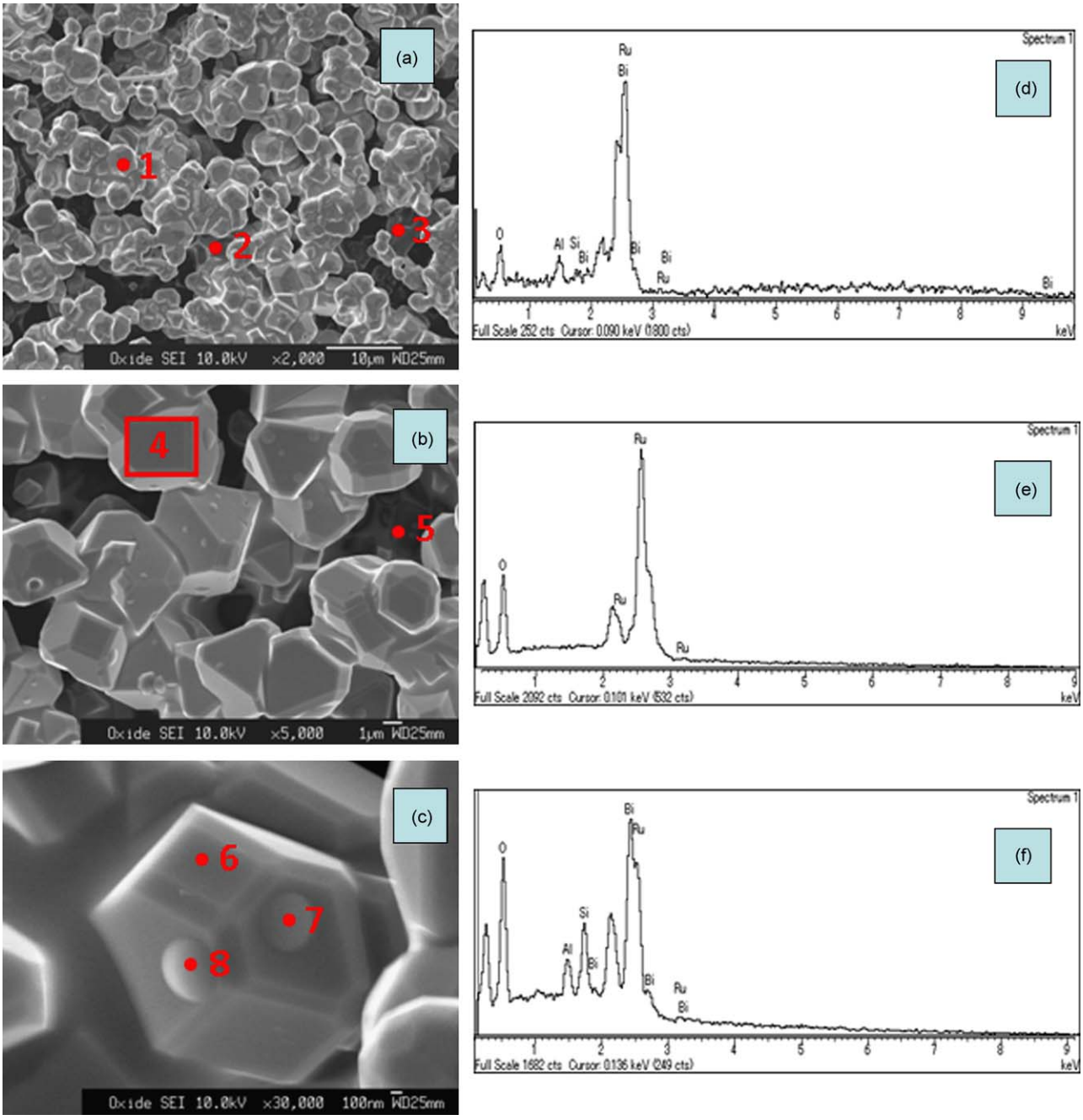

Fig. 4. SEM images at different magnification of $Bi_2Ru_2O_{7+x}$ + RuO_2-SE showing complexity of SE structure (a–c); EDX spectra for points 1, 4 and 6 (d); EDX spectra for points 2, 3 and 5 (e); EDX spectra for points 7 and 8 (f).

Fig. 4(a)–(c) exhibits SEM micrographs for the surface morphology for the $Bi_2Ru_2O_{7+x} + RuO_2$ film sintered at 965 °C. Fig. 4(d)–(f) illustrates EDX spectra for appropriate points on the SEM images. The film SE sintered at such temperature consists of homogeneous quasi-spherical RuO_2 grains with an average size of about ~1 μm. The grain formation is not compact since many pores were estimated at about 1–3 μm, over large areas. EDX measurement further confirmed the development of two independent phases: $Bi_2Ru_2O_{7+x}$ and RuO_2. The structure of this SE provides high surface-to-volume ratio and consequently large number of adsorption centres on the surface of SE for pH and DO measurements. Active surface sites on the edges of these sub-micron particles are especially desirable for surface reactions with DO in water. Noteworthy, RuO_2 nanostructures have shown a hydrophobic character of their surfaces [15]. As a result, although this SE is relatively porous, water does not diffuse inside the electrode structure. Our previous results of *in situ* FTIR RuO_2 measurements [18] also confirmed that the active sites for the oxygen reduction (oxygen adsorption) are not limited to the triple boundaries but extended to surfaces of RuO_2.

Ceramic water quality sensors attached with $Bi_2Ru_2O_{7+x}$ + RuO_2-SE have been extensively tested for pH measurements during 18 months. Potentiometric measurement of pH revealed that for the thick-film sensor exhibited an excellent reproducibility in pH measurement from strong acid (2.0 pH) to strong alkaline (13.0) solutions. The Nernstian slope was 58 mV/pH at 23 °C versus Ag/AgCl-RE. An excellent agreement between the Nernstian slopes for the different $Bi_2Ru_2O_{7+x}$ + RuO_2-SEs of the sensors was obtained. The data was closely followed a straight line suggesting that only one electron per oxygen molecule was involved. This could be related to the existence of superoxide ions and the following electrochemical reaction [19,20]:

$$O_{2,aq} + e^- \leftrightarrow O_2{}^-{}_{,ads}$$

The standard deviation of the output *emf* was found to be around ±7 mV within the whole pH measurement range. It was considered as an improvement to the previously published standard deviation ±30–50 mV for the Ru-containing electrode paste [9]. This is apparently due to the improvement of the SE structure and the absence of lead in the SE. The reproducibility of the test results between different days when the measurements were carried out was found to be ±2 mV. The results obtained in this study were in very good agreement with recently published results of using RuO_2 nanostructures and carbon nano-tubes in pH sensor [20].

Selectivity measurements revealed that the presence of Ca^{2+}, NO_3^- and SO_4^{2-} has no effect on the sensor *emf*. Changes of Cl^- concentration from 10^{-7} mol/l to 10^{-2} mol/l shown that Cl^- ions have very small impact on the sensor output. Moreover, presence of Li^+, Na^+, K^+, Mg^{2+} from 10^{-5} mol/l to 10^{-2} mol/l changes the measuring potential on approximately ±5%, but does not have any significant impact on the pH potential slope.

Typical data for response/recovery time for the water quality sensor attached with $Bi_2Ru_2O_{7+x}$ + RuO_2-SE is presented in Fig. 5(a). It should be noted that in warm water the sensor's response to pH changes was much faster than in cold water. For the freshly prepared $Bi_2Ru_2O_{7+x}$ + RuO_2-SE the response/recovery time was within seconds in working temperature range of 20–30 °C. However, it was slower than the response/recover time for nanostructured RuO_2-SE [13,15,20]. Considering that pH measurements are required not only in warm, but also in cold water, dynamic characteristics of the $Bi_2Ru_2O_{7+x}$ + RuO_2-SE were also studied at a temperature range of 4–20 °C. The results obtained confirm that the operating temperature influences the response and recovery rate significantly: the response and recovery time decreases with the decrease of temperature. Although the absolute value of *emf* for pH measurements drifted to lower value in time, the response time remained reasonably fast during all experiments. Fig. 5(b) summarises typical response transients to pH changes at different working temperatures for both freshly prepared $Bi_2Ru_2O_{7+x}$ + RuO_2-SE and $Bi_2Ru_2O_{7+x}$ + RuO_2-SE after their 12 months use in the water quality sensor. Although the

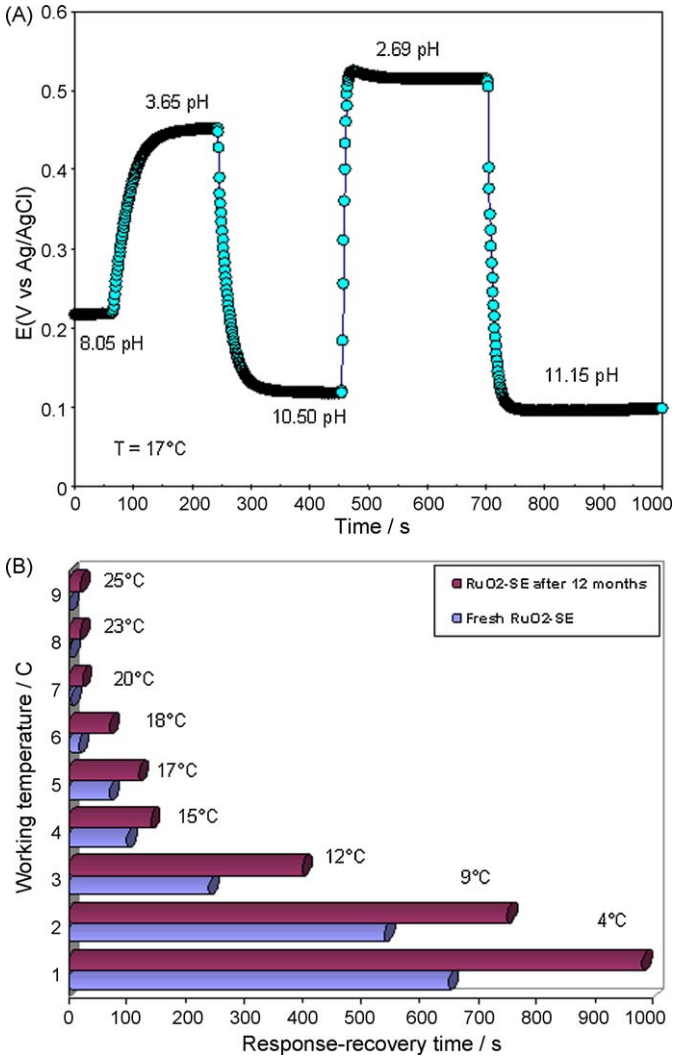

Fig. 5. Dynamic characteristics of nanostructured $Bi_2Ru_2O_{7+x}$ + RuO_2-SE in aqueous solution vs. a Ag/AgCl-RE at pH changes at a temperature of 17 °C (a) and summary of response/recovery time for both freshly prepared $Bi_2Ru_2O_{7+x}$ + RuO_2-SE and $Bi_2Ru_2O_{7+x}$ + RuO_2-SE after use for 12 months (b).

response/recovery rate was about ~10–12 min in the coldest measured temperatures, owing to the nature of the water quality monitoring (24 h per day) the adequate information about the changes in water quality can be obtained and analysed. The data presented in Fig. 5(b) also revealed that the response/recovery rates for the $Bi_2Ru_2O_{7+x}$ + RuO_2-SE used for 12 months are more sluggish due to possible biofouling effect, which will be discussed later.

The DO measuring characteristics of the sensor using $Bi_2Ru_2O_{7+x}$ + RuO_2-SE at different pHs and a working temperature of 19 °C are shown in Fig. 6. The *emf* values were almost linear to the logarithm of DO concentration at each temperature examined. The present sensor is able to detect DO in the concentration range of 0.5–8.0 ppm. It is noted that the DO sensitivity is the highest at neutral pH.

Long-term stability trial of the ceramic sensor attached with $Bi_2Ru_2O_{7+x}$ + RuO_2-SE has been carried out for more than 18 months in order to find out the sensor's durability without

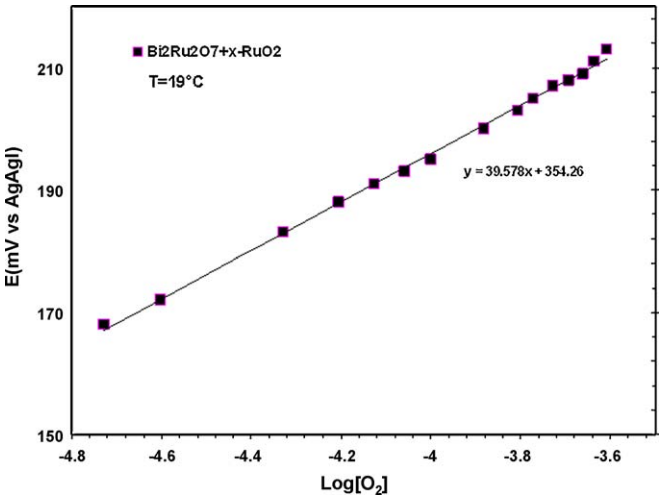

Fig. 6. Typical DO characteristics of the electrochemical sensor using $Bi_2Ru_2O_{7+x}$ + RuO_2-SE at a measuring temperature of 19 °C.

degradation of the output *emf*. This sensor was involved into continuous pH measurement at the temperature of 20 °C and the results of this trial are shown in Fig. 7. Substantial *emf* drift during the first month of the testing was due to the H^+ transport through SE, which is governed by dissolved H_2 trapping at the trap sites existing at the grain boundaries or micro-pores of the nanostructured $Bi_2Ru_2O_{7+x}$ + RuO_2-SE [5,14]. Therefore, all sensors in this study were conditioned in water at 23 °C for 15 days before any meaningful results of the pH measurements were made. After stabilization, the output *emf* remained stable during the following months of testing, showing a standard drift about ±1.5 mV/month. After about 11 months of the long-term stability trial, the output *emf* started to show significant decrease. The observed decrease in the sensor output signal is likely to be caused by to bio-fouling effect. There is no doubt that the bio-fouling started to accumulate on the SE grains probably after a couple of months of testing. However, the significance of this process has become visible on the output *emf* drift after about 11 months and it seems to increase as about

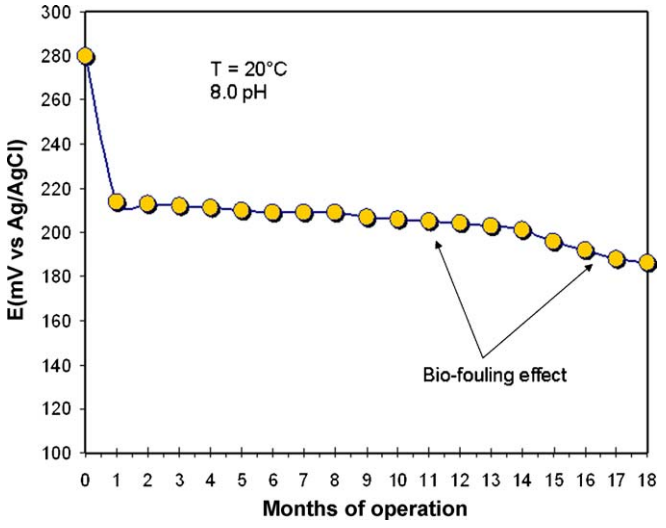

Fig. 7. Long-term stability testing of $Bi_2Ru_2O_{7+x}$ + RuO_2-SE.

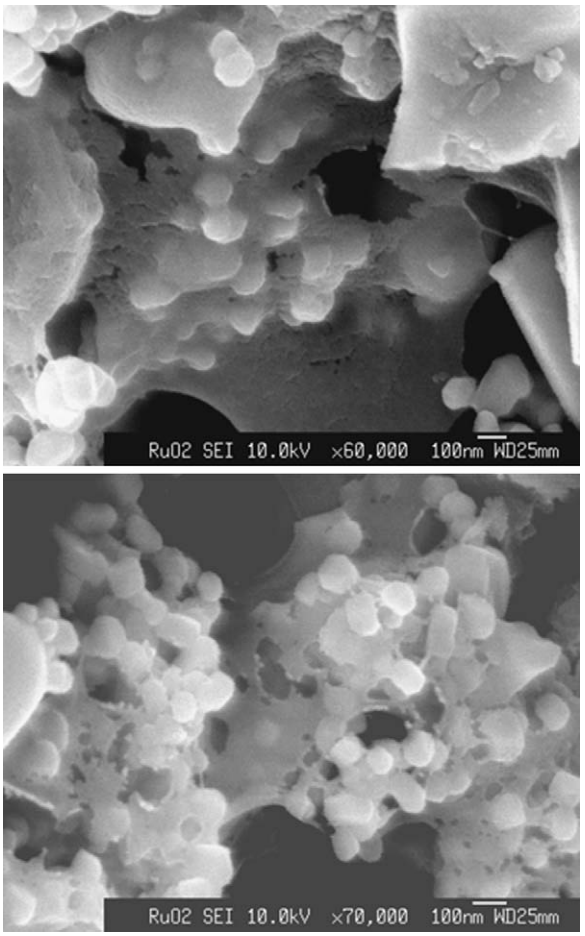

Fig. 8. SEM images of the $Bi_2Ru_2O_{7+x}$ + RuO_2-SE after 11 months of long-term stability trial.

14 months. Fig. 8 shows the SEM images of nanostructured $Bi_2Ru_2O_{7+x}$ + RuO_2-SE after 11 months of service in water at the temperature of 20 °C.

It is clearly shown that bio-fouling deposited on $Bi_2Ru_2O_{7+x}$ + RuO_2-SE covers $Bi_2Ru_2O_{7+x}$ + RuO_2 nano-particles and consequently changes the sensor characteristics. This bio-fouling is likely to consist of bacteria and algae, as a typical bio-fouling in water [21]. Considering that the long-term stability trial of the sensor attached with $Bi_2Ru_2O_{7+x}$ + RuO_2-SE was organised in the fresh water, the bio-fouling effect would have much more significant impact on the sensor characteristics, if the sensor is intended to be used in wastewater. Therefore, the development of the means of bio-fouling resistance is mandatory for successful implementation of the above sensor into wide practical use. One of the effective ways to increase bio-fouling resistance is doping of RuO_2 by another nano-oxide possessing significant anti-fouling resistance [22].

Development of the multi-sensor capable to accurately measure the main water quality parameters: pH, DO, temperature, conductivity and turbidity will provide an opportunity for analysis of water quality. Recently developed CSIRO software provides a suitable graphic user interface interactive and with information on screen. The advantage of this software is that it allows, with minimum time and with no

need to be an expert programmer, quick modifications, data acquisition, calculation and data management. The program makes necessary calculations to obtain the parameters (pH, turbidity, DO, etc.) from the sensor's readings. The program makes a sequential sweeping of all inputs, accepting the selection of sampling frequency at any time (1 s by default). In order to facilitate the analysis of results a temporal mark, indicating the day, hour and second of the acquisition is inserted in the file.

4. Conclusions

A new type of ceramic multi-sensor for water quality analysis based on sub-micron $Bi_2Ru_2O_{7+x}$ + RuO_2-SE is presented. The measurement of the main parameters of water quality such as pH, DO, conductivity, temperature and turbidity are the main areas of application for these sensors. In contrast to the laboratory analytical instruments used for water quality analysis, the alternative solid-state sensors are less expensive, accurate and can be combined into the wireless sensor networks covering large areas of water quality monitoring. These thick-film sensors are fully compatible with conventional microelectronic batch processes. Although the presented sensors have been shown to be an excellent sensing platform for water quality control, these instruments have yet to be tested in the real industrial environments to demonstrate that they are suitable for use by industry. Utilizing new semiconductor nanostructured materials for SE will allow extending the sensitivity properties of all-solid-state film micro-sensors and micro-sensor arrays and consequently problems solved by materials science. Further studies are needed to provide necessary mean for protection of SE from bio-fouling, since the bio-fouling can be one of the main destructive factors during deployment of these sensors into the real industrial applications.

Acknowledgements

This work was partially supported by Research and Development Program of CSIRO Sensors and Sensor Networks Transformation Capability Platform and CSIRO Materials Science and Engineering Division—project ''Water Quality Sensors''. The author wishes to thank Research Director of CSIRO SSN TCP Dr. Michael Brünig for useful discussions.

References

[1] H.N. McMurray, P. Douglas, D. Abbot, Novel thick-film pH sensor based on ruthenium dioxide-glass composites, Sens. Actuators B 28 (1995) 9–15.
[2] J.K. Atkinson, A.W. Cranny, W.V. Glasspool, J.A. Mihell, An investigation of the performance characteristics and operational lifetimes of multi-element thick film sensor arrays used in the determination of water quality parameters, Sens. Actuators B 54 (1999) 215–231.
[3] L.A. Pocrifka, C. Goncalves, P. Grossi, P.C. Colpa, E.C. Pereira, Development of RuO_2–TiO_2 (70–30) mol% for pH measurements, Sens. Actuators B 113 (2006) 1012–1016.
[4] P. Kurzweil, Precious metal oxides for electrochemical energy converters: pseudocapacitance and pH dependence of redox processes, J. Power Sources 190 (2009) 189–200.
[5] Y.-H. Liao, J.-C. Chou, Preparation and characteristics of ruthenium dioxide for pH array sensors with real-time measurement system, Sens. Actuators B 128 (2008) 603–612.
[6] R.D. Prien, The future of chemical in situ sensors, Mar. Chem. 107 (2007) 422–432.
[7] G.A.E. Mostafa, Development and characterization of ion selective electrode for the assay of antimony, Talanta 71 (2007) 1449–1454.
[8] L. Moreno, A. Merlos, N. Abramova, J. Jimenez, A. Bratov, Multi-sensor array as an ''electronic tongue'' for mineral water analysis, Sens. Actuators B 116 (2006) 130–134.
[9] R. Matinez-Manez, J. Soto, E. Garcia-Breijo, L. Gil, J. Ibanez, E. Gadea, A multisensor in thick-film technology for water quality control, Sens. Actuators B 120 (2005) 589–595.
[10] R. Martinez-Manez, J. Soto, J. Lizondo-Sabater, E. Garcia-Breijo, L. Gil, J. Ibanez, I. Alcaina, S. Alvarez, New potentiometric dissolved oxygen sensors in thick film technology, Sens. Actuators B 101 (2004) 295–301.
[11] R. Matinez-Manez, J. Soto, E. Garcia-Breijo, L. Gil, J. Ibanez, E. Llobet, An ''electronic tongue'' design for the qualitative analysis of natural waters, Sens. Actuators B 104 (2005) 302–307.
[12] R.-H. Labrador, J. Soto, R. Martinez-Manez, C. Coll, A. Benito, J. Ibanez, E. Garcia-Breijo, L. Gil, An electrochemical characterization of thick-film electrodes based on RuO_2-containing resistive pastes, J. Electroanal. Chem. 611 (2007) 175–180.
[13] S. Zhuiykov, Morphology and sensing characteristics of nanostructured RuO_2 electrodes for integrated water quality monitoring sensors, Electrochem. Commun. 10 (2008) 839–843.
[14] S. Zhuiykov, Morphology of Pt-doped nanofabricated RuO_2 sensing electrodes and their properties in water monitoring sensors, Sens. Actuators B 136 (2009) 248–256.
[15] S. Zhuiykov, D. O'Brien, M. Best, Water quality assessment by an integrated multi-sensor based on semiconductor RuO_2 nanostructures, Meas. Sci. Technol. 20 (2009) 095201.
[16] On the restriction of use certain hazardous substances in electrical and electronic equipment (ROHS); directive 2002/95/EC of the European Parliament and of the Council, 2002.
[17] S. Zhuiykov, WO 2009/135270 A1 PCT, A composite material for use in a sensing electrode for measuring water quality, November 12, 2009.
[18] S. Zhuiykov, In situ FTIR study of oxygen adsorption on nanostructured RuO_2 thin-film electrode, Ionics 15 (2009) 507–512.
[19] S. Zhuiykov, Potentiometric DO detection in water by ceramic sensor based on sub-micron RuO_2 sensing electrode, Ionics 15 (2009) 693–701.
[20] B. Xu, W.D. Zhang, Modification of vertically aligned carbon nanotubes with RuO_2 for a solid-state pH sensor, Electrochim. Acta 55 (2010) 2859–2864.
[21] D.M. Yebra, S. Kiil, K. Dam-Johansen, Antifouling technology—past, present and future steps towards efficient and environmentally friendly antifouling coatings, Prog. Org. Coat. 50 (2004) 75–104.
[22] S. Zhuiykov, E. Kats, D. Marney, Development Cu_2O-doped RuO_2 sensing electrode of water sensor with improved antifouling resistance, Talanta 82 (2010) 502–507.